This article is a *Plant Cell* Advance Online Publication. The date of its first appearance online is the official date of publication. The article has been edited and the authors have corrected proofs, but minor changes could be made before the final version is published. Posting this version online reduces the time to publication by several weeks.

Auxin Depletion from the Leaf Axil Conditions Competence for Axillary Meristem Formation in *Arabidopsis* and Tomato[W][OPEN]

Quan Wang,[a] Wouter Kohlen,[a] Susanne Rossmann,[a] Teva Vernoux,[b] and Klaus Theres[a,1]

[a] Max Planck Institute for Plant Breeding Research, D-50829 Cologne, Germany
[b] Laboratoire de Reproduction et Développement des Plantes, CNRS, INRA, ENS Lyon, UCBL, Université de Lyon, 69364 Lyon, France

ORCID ID: 0000-0003-2912-1263 (Q.W.)

The enormous variation in architecture of flowering plants is based to a large extent on their ability to form new axes of growth throughout their life span. Secondary growth is initiated from groups of pluripotent cells, called meristems, which are established in the axils of leaves. Such meristems form lateral organs and develop into a side shoot or a flower, depending on the developmental status of the plant and environmental conditions. The phytohormone auxin is well known to play an important role in inhibiting the outgrowth of axillary buds, a phenomenon known as apical dominance. However, the role of auxin in the process of axillary meristem formation is largely unknown. In this study, we show in the model species *Arabidopsis thaliana* and tomato (*Solanum lycopersicum*) that auxin is depleted from leaf axils during vegetative development. Disruption of polar auxin transport compromises auxin depletion from the leaf axil and axillary meristem initiation. Ectopic auxin biosynthesis in leaf axils interferes with axillary meristem formation, whereas repression of auxin signaling in polar auxin transport mutants can largely rescue their branching defects. These results strongly suggest that depletion of auxin from leaf axils is a prerequisite for axillary meristem formation during vegetative development.

INTRODUCTION

Shoot and inflorescence architecture of flowering plants is largely based on the activity of meristems. During embryogenesis, two groups of pluripotent cells are established: the shoot apical meristem (SAM) and the root apical meristem (Laux and Jurgens, 1997). In the postembryonic phase of development, the root apical meristem will form the entire root system, whereas the SAM will produce the aerial organs by continuous addition of growth units, called phytomeres, which normally consist of three parts: an internode, a leaf, and an axillary meristem (AM), formed in the leaf axil (Evans and Grover, 1940). The number and activity of AMs determine to a large extent plant fitness and crop yield.

During vegetative development, leaves are initiated in a regular pattern from cells at the flanks of the SAM. Transport of the mobile phytohormone auxin in the epidermal layer (L1 layer) of the SAM leads to the formation of auxin maxima, which determines the positions of leaf initiation (Reinhardt et al., 2003). In *Arabidopsis thaliana*, the most important transporter related to auxin distribution in the SAM is the auxin efflux carrier PIN-FORMED1 (PIN1). In the absence of PIN1 activity, *Arabidopsis* meristems form only few lateral organs resulting in a pin-like stem architecture (Okada et al., 1991). *PIN1* encodes a transmembrane protein (Gälweiler et al., 1998) that is highly expressed in the L1 layer of the SAM and in the vascular system (Reinhardt et al., 2003; Bayer et al., 2009). Polar PIN1 protein localization within a cell directs the auxin flow to convergence points resulting in auxin accumulation and response maxima, which are required for leaf primordium initiation (Reinhardt et al., 2003). After the formation of leaves, AMs are initiated in the axils of these leaves. AMs develop into vegetative and inflorescence branches, as well as into floral primordia (Schmitz and Theres, 2005). Timing of AM initiation and their further development are strongly influenced by the developmental status of the plant. During prolonged vegetative development in *Arabidopsis*, AMs are initiated in an acropetal gradient at a distance to the main shoot meristem (Hempel and Feldman, 1994; Stirnberg et al., 1999; Grbić and Bleecker, 2000; Stirnberg et al., 2002). However, in the reproductive stage, axillary branches are initiated evenly (Stirnberg et al., 1999, 2002) or in a basipetal sequence (Hempel and Feldman, 1994) at close proximity to the SAM. Similarly, floral meristems emerge very rapidly at the flanks of the SAM (Heisler et al., 2005).

Characterization of mutants defective in axillary bud formation identified important regulators of AM development. The orthologous GRAS-domain transcription factors LATERAL SUPPRESSOR (Ls) from tomato (*Solanum lycopersicum*) (Schumacher et al., 1999) and LATERAL SUPPRESSOR (LAS) from *Arabidopsis* (Greb et al., 2003), as well as MONOCULM1 (MOC1) from rice (*Oryza sativa*; Li et al., 2003), control AM initiation. Mutations in Ls/LAS cause strong defects in AM formation, leading to loss of side shoots during vegetative development in tomato and *Arabidopsis* (Schumacher et al., 1999; Greb et al., 2003). Loss of MOC1 function results in a lack of tillers as well as in a reduction of reproductive rachis branches and spikelets (Li et al., 2003). *Ls/LAS/MOC1* are expressed in the boundary zones between the SAM and leaf primordia (Schumacher et al., 1999; Li et al., 2003; Busch et al., 2011), where new meristems are initiated. These specific expression patterns are similar to those of the *CUP-SHAPED COTYLEDON* genes (*CUC*) (Aida et al., 1997,

[1] Address correspondence to theres@mpipz.mpg.de.
The author responsible for distribution of materials integral to the findings presented in this article in accordance with the policy described in the Instructions for Authors (www.plantcell.org) is: Klaus Theres (theres@mpipz.mpg.de).
[W] Online version contains Web-only data.
[OPEN] Articles can be viewed online without a subscription.
www.plantcell.org/cgi/doi/10.1105/tpc.114.123059

1999; Takada et al., 2001; Vroemen et al., 2003; Hibara et al., 2006), which regulate embryonic SAM development and boundary zone establishment. In addition, CUC1, CUC2, and CUC3 modulate AM initiation redundantly (Hibara et al., 2006; Raman et al., 2008).

In the vegetative phase of development, newly established AMs produce a few leaves forming an axillary bud. These buds either remain dormant or grow out depending on internal and external cues. In many plant species, the outgrowth of axillary buds is inhibited by an active apical bud, generally referred to as apical dominance. Auxin (Thimann and Skoog, 1934) and strigolactones (Gomez-Roldan et al., 2008; Umehara et al., 2008) have been identified as important signals in a regulatory network modulating the outgrowth of axillary buds. In the auxin signaling mutant *auxin resistant1* (*axr1*), axillary buds are partially resistant to the inhibitory effect of auxin, resulting in an enhanced outgrowth during both vegetative and reproductive development (Lincoln et al., 1990; Leyser et al., 1993; Stirnberg et al., 1999).

In maize (*Zea mays*) inflorescence development, the phytohormone auxin was also demonstrated to play an important role in reproductive AM formation. Application of the auxin efflux carrier inhibitor *N*-1-naphthylphthalamic acid (NPA) not only inhibits the initiation of AMs in the maize inflorescence, but also affects spikelet development (Wu and McSteen, 2007). AM formation is strongly compromised in the polar auxin transport mutant *barren inflorescence2* (*bif2*) (McSteen and Hake, 2001; McSteen et al., 2007). *BIF2* encodes an AGC Ser/Thr kinase and is the ortholog of the *Arabidopsis PINOID* (*PID*) protein. PID was shown to regulate the intracellular localization of the PIN auxin efflux carriers, which directs auxin flux (Friml et al., 2004; Michniewicz et al., 2007).

In this study, the role of auxin in vegetative AM formation was investigated in *Arabidopsis* and tomato. We show that a block in polar auxin transport leads to a defect in AM formation. By monitoring PIN1 localization and using different auxin signaling reporters, we demonstrate that auxin is depleted from the boundary between a leaf primordium and the SAM, establishing a low auxin zone. Ectopic auxin biosynthesis in leaf axils interferes with axillary meristem formation, whereas repression of auxin signaling in polar auxin transport mutants can largely rescue their branching defects. These results strongly suggest that the low auxin signaling in leaf axils is crucial for axillary meristem formation during vegetative development.

RESULTS

Auxin Transport Is Required for Axillary Meristem Formation

To investigate the role of auxin in AM formation, the shoot branching phenotypes of the auxin influx and efflux transport mutants were analyzed. In *Arabidopsis* vegetative shoot apices, the major auxin influx carriers are AUXIN RESISTANT1 (AUX1), LIKE-AUX1 (LAX1), and LAX2 (Bainbridge et al., 2008), whereas the main auxin efflux carrier is PIN1 (Reinhardt et al., 2003; Vernoux et al., 2010). In comparison to Columbia-0 (Col-0) wild-type plants (Figure 1A), both *aux lax1 lax2* triple and *pin1* mutants were found to be strongly compromised in axillary bud development (Figure 1B). Many rosette leaf axils of the *aux lax1 lax2* triple mutant, especially late rosette leaf axils, did not form axillary buds and occasionally cauline leaf axils were empty as well (Figure 1B). The *pin1* mutant, which develops a pin-like inflorescence, produced much less leaves than the wild type (Figures 1A and 1C) and almost none of the leaf axils formed a bud (Figure 1D). The branching defects in

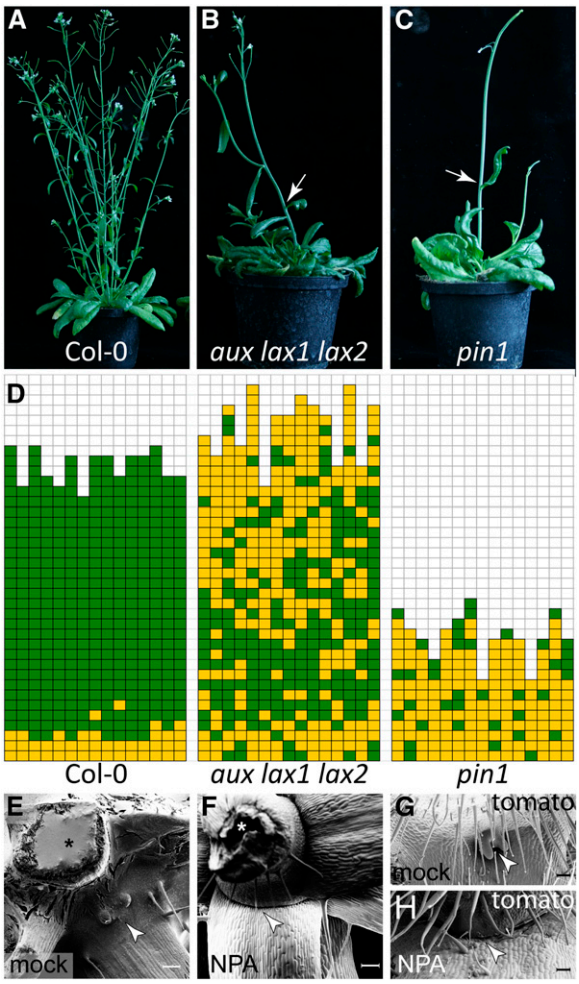

Figure 1. Auxin Transport Is Required for Axillary Meristem Formation.

(A) to **(C)** Growth habit of a Col-0 wild type **(A)**, an *aux lax1 lax2* triple mutant **(B)**, and a *pin1* mutant **(C)** plant. Arrows in **(B)** and **(C)** point to empty cauline leaf axils.

(D) Schematic representation of axillary bud formation in rosette leaf axils of Col-0, *aux lax1 lax2*, and *pin1* (n = 15). Each column represents a single plant, and each square within a column indicates an individual leaf axil. The bottom row represents the oldest rosette leaf axils, with positions of progressively younger rosette leaves on top of it. Green denotes the presence of an axillary bud and yellow the absence of an axillary bud in any particular leaf axil.

(E) and **(F)** Micrograph of the top rosette leaves of a Col-0 wild-type plants grown on MS medium with mock treatment **(E)** and MS medium containing 10 μM NPA **(F)**. Arrowhead points to an axillary bud **(E)** and an empty leaf axil **(F)**. Asterisk indicates the main stem. Plants were grown under SD for 4 weeks and then shifted to LD to induce flowering.

(G) and **(H)** Micrograph of a tomato (cv Moneymaker) leaf axil mock treated **(G)** or treated with 10 μM NPA **(H)**. Arrowhead points to an axillary bud **(G)** and an empty axil **(H)**. Bars = 200 μm in **(E)** to **(H)**.

auxin efflux– and auxin influx–related mutants suggest that auxin transport is required for AM formation in *Arabidopsis*.

To test this hypothesis, the polar auxin transport inhibitor NPA was used to chemically block auxin transport. On Murashige and Skoog (MS) medium without NPA (mock), *Arabidopsis* seeds germinated readily and axillary buds became visible after induction of flowering (Figure 1E). However, on MS medium containing 10 μM NPA, Col-0 wild-type plants displayed severe growth defects. Germination was strongly reduced, and after induction of flowering (long-day [LD] conditions), ~20% of the plants formed a pin-like inflorescence, phenocopying the *pin1* mutant (Figure 1C). Axillary bud formation was strongly reduced in NPA-treated plants in comparison to control plants, especially in late rosette leaf axils. Scanning electron microscope imaging of empty leaf axils did not uncover any morphological structure resembling an axillary bud (Figure 1F).

To explore whether NPA treatment induces similar defects in shoot architecture in different plant species, tomato plants (cv Moneymaker) were grown on MS medium containing NPA. NPA-treated tomato plants showed a dwarf growth habit and dark green leaf color. Furthermore, several of these NPA-treated plants prematurely stopped shoot development with a pin-like inflorescence (Supplemental Figure 1), similar to NPA-treated *Arabidopsis*. In contrast to mock-treated tomato plants, which produced axillary buds from all leaf axils (Figure 1G), NPA-treated plants developed several empty leaf axils (Figure 1H). In addition, several phenotypes previously associated with NPA application (Koenig et al., 2009) were also observed in our experiments (e.g., fewer leaves, strong reduction in the number of leaflets, and a round leaf margin; Supplemental Figure 1). The phenotype of these NPA-treated plants confirmed that polar auxin transport is mandatory for axillary bud formation.

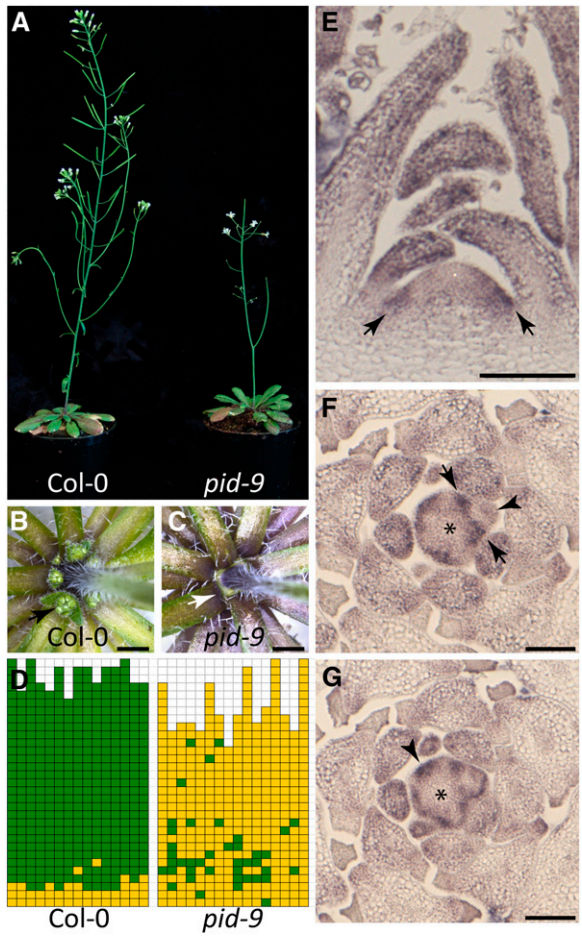

Figure 2. PID Modulates Axillary Bud Formation during Vegetative *Arabidopsis* Development.

(A) Growth habit of Col-0 wild type (left) and *pid-9* mutant (right).
(B) and **(C)** Close-up views of top rosette leaf axils of a Col-0 **(B)** and a *pid-9* **(C)** plant. Arrow points to an axillary bud in **(B)** and an empty leaf axil in **(C)**. Bars = 2 mm.
(D) Schematic representation of axillary bud formation in rosette leaf axils of Col-0 (n = 15, same population as in Figure 1D) and *pid-9* mutants (n = 16). Plants were grown under SD for 4 weeks and then shifted to LD to induce flowering.
(E) to **(G)** RNA in situ hybridization analysis of the pattern of *PID* transcript accumulation in Col-0 wild-type shoot apices from 28-d-old SD grown plants. Medial longitudinal **(E)** and two 8-μm consecutive transverse (**[F]** and **[G]**) sections were hybridized to a *PID* antisense probe. Arrows indicate *PID* expression in the peripheral zone of the SAM **(E)**, in the leaf axil **(F)**, and in a newly formed leaf primordium **(G)**. Arrowhead in **(F)** points to a young leaf primordium where *PID* expression was downregulated. Asterisks indicate the SAM. Bars = 100 μm.

PID Modulates Axillary Meristem Formation

The AGC III kinase PID was proposed to modulate polar auxin transport by regulating PIN1 localization within the cell (Friml et al., 2004; Michniewicz et al., 2007). In addition, PID regulates boundary zone establishment and apical patterning during embryogenesis (Furutani et al., 2004). To test for a possible role of PID in AM formation during vegetative shoot development, we characterized the pattern of axillary bud formation in *pid* mutants. Like the *pin1* mutant, plants homozygous for the strong *pid-9* allele developed a pin-like inflorescence, which was sterile (Figure 2A). Most rosette leaf axils of *pid-9* plants failed to form axillary buds (Figures 2C and 2D), while Col-0 wild-type plants produced axillary buds in all rosette leaf axils, with the exception of the early vegetative leaf axils (Figures 2B and 2D). Plants carrying the weak *pid-8* allele were also strongly compromised in axillary bud formation and showed abnormal phyllotaxis and flower development (Supplemental Figure 2).

To correlate PID function with the process of AM formation, *PID* expression in the vegetative *Arabidopsis* shoot apex was analyzed by RNA in situ hybridization. Longitudinal sections revealed *PID* mRNA accumulation in the periphery of the vegetative SAM (Figure 2E). Transverse sections showed more clearly that *PID* mRNA accumulated to higher levels in the peripheral zone of the SAM (Figure 2F) and in newly formed leaf primordia (Figure 2G, arrowhead). In slightly older primordia, *PID* expression was focused to the boundary region between the SAM and the primordium (Figure 2F, between arrows) and no longer detectable in the bulk of the primordium (Figure 2F, arrowhead).

Long and Barton (2000) have shown that *SHOOT MERISTEMLESS* (*STM*) expression can be used as an early marker for AM initiation. To further characterize the defect in axillary bud

formation, *STM* mRNA accumulation was monitored in wild-type and *pid-9* plants. Transverse sections through shoot tips of vegetative plants were hybridized with an *STM* antisense probe. *STM* was highly expressed in the SAM and in the interprimordial regions of both wild-type and *pid-9* plants (Figures 3A and 3B, arrows; Supplemental Figures 3A and 3B). In the axils of older leaf primordia of Col-0, *STM* mRNA accumulated in a group of small cells next to the adaxial center of the primordium boundary (Figure 3A, arrowhead; Supplemental Figures 3A and 3B). However, this focused *STM* expression was not found in *pid-9* (Figure 3B, arrowhead). The absence of the focused *STM* signal in mature leaf axils of *pid-9* plants suggested that AMs were not initiated in *pid-9* during vegetative development.

The strong defects in axillary bud formation observed in *pid-9* mutants could be correlated with or result from the loss of gene activities involved in the regulation of AM formation. To test this hypothesis, expression of the boundary-specific gene *LAS* was monitored. Similar to the wild type, *LAS* mRNA accumulated at the boundary between the SAM and young leaf primordia (Figures 3C and 3D; Supplemental Figure 3C). Identical *LAS* expression patterns in both the wild type and *pid-9* suggest that boundary formation is maintained and the branching defects in *pid-9* are unlikely due to a change in *LAS* expression.

In addition, we tested whether branching defects in *pid-9* were due to alterations in meristem organization or leaf initiation. Meristem organization and leaf primordium formation in *pid-9* were analyzed by in situ hybridization using the organizing center-specific gene *WUSCHEL* (*WUS*) (Mayer et al., 1998) and the leaf identity gene *MONOPTEROS* (*MP*) (Hardtke and Berleth, 1998) as probes. In *pid-9*, the *WUS* expression pattern did not exhibit any alteration in comparison to Col-0 (Figures 3E and 3F), suggesting that SAM organization was not disrupted. *MP* encodes an auxin response factor that is expressed at the positions of incipient leaf primordia (Hardtke and Berleth, 1998). *MP* transcript accumulation in vegetative *pid-9* shoot apices did not deviate from the wild type (Figures 3G and 3H), as also observed in inflorescence apices (Christensen et al., 2000). *MP* mRNA also accumulated to high levels in the provascular elements of both the wild type and *pid-9* (Figures 3G and 3H). Similar expression patterns of *WUS* and *MP* in the wild type and *pid-9* mutants indicate that the observed branching defects in *pid-9* are not a consequence of an alteration in meristem organization or leaf initiation.

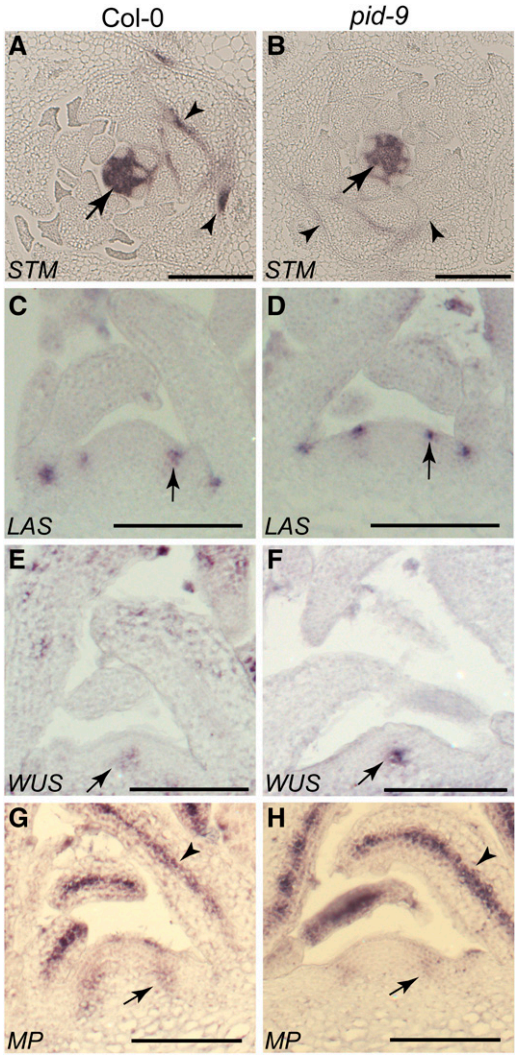

Figure 3. Axillary Meristems Fail to Initiate in *pid-9* Mutants.

Transverse (**[A]** and **[B]**) and longitudinal (**[C]** to **[H]**) sections through vegetative shoot apices of Col-0 wild-type and *pid-9* mutant plants were hybridized to different antisense probes (indicated on the bottom left corner).
(A) and **(B)** *STM* mRNA was detected in the SAM and in interprimordial regions (arrows). However, a focused *STM* expression domain was observed close to the adaxial center of older leaf primordia of the wild type (**[A]**, arrowheads) but not in the *pid-9* mutant (**[B]**, arrowheads). Bars = 200 μm.
(C) and **(D)** *LAS* mRNA accumulated in the boundary zone between young leaf primordia and the meristem/stem (arrows).
(E) and **(F)** *WUS* expression was detected in the organizing center of the SAM (arrows).
(G) and **(H)** *MP* transcripts accumulated in incipient leaf primordia (arrow) and in the provascular system (arrowhead). Materials were harvested from plants grown under SD for 28 d. Bars = 100 μm in **(C)** to **(H)**.

PIN1 Distribution in Tomato and *Arabidopsis* Shoot Apices

As polar auxin transport is required for AM formation, the distribution and intracellular polarization of the major auxin efflux carrier PIN1 in the shoot apex may indicate the direction of auxin flow in the leaf axil (Reinhardt et al., 2003; Heisler et al., 2005). For this purpose, we first used tomato, which offers the advantage that PIN1 distribution in the shoot apex can be easily monitored by confocal microscopy. In tomato, AMs initiate in the axils of P6/7 leaf primordia (Supplemental Figure 4). To monitor PIN1 distribution in the boundary zone of leaf primordia, plants harboring an *AtPIN1:PIN1:GFP* (Bayer et al., 2009) construct were used. As shown in Figure 4A, PIN1 was found to be highly expressed in incipient leaf primordia and in the L1 layer of both the SAM and young leaf primordia. In addition, PIN1 accumulated to high levels at the tip of young leaves and in their leaf provascular system. Interestingly, the PIN1 level was low in the axils of young leaf primordia (Figure 4B). In the vicinity of the axillary boundary zone, PIN1 proteins were polarized toward the shoot apex and the leaf primordium tip, indicating that auxin was likely depleted from leaf axils by these PIN1 proteins (Supplemental Figures 5A and 5B).

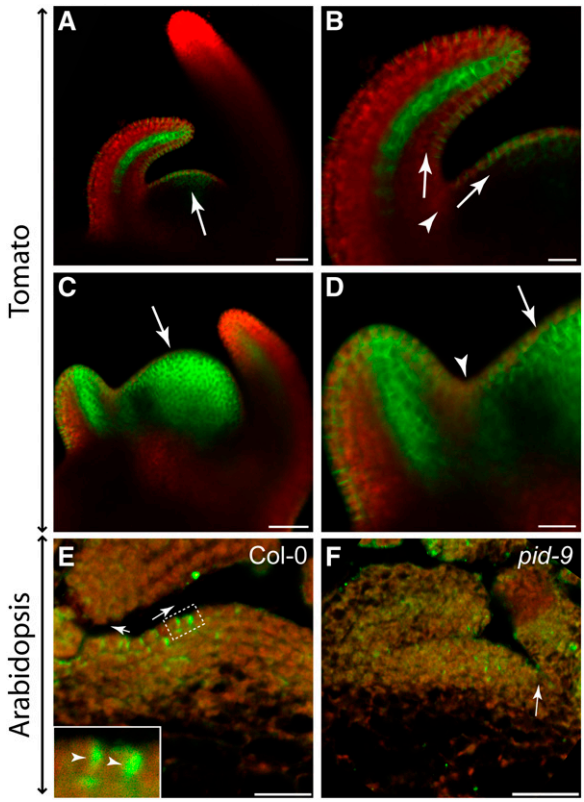

Figure 4. PIN1 Distribution in Tomato and *Arabidopsis* Vegetative Shoot Apices.

(A) to **(D)** PIN1 distribution in vegetative shoot apices of transgenic tomato plants (cv Moneymaker).

(A) Confocal image of a transgenic *AtPIN1:PIN1:GFP* tomato apex after mock treatment. Arrow points to an incipient leaf primordium.

(B) Close-up of axillary region of the shoot apex shown in **(A)**. PIN1 protein localization was detected in the epidermis, suggestive of an auxin flow out of the axillary region (arrows) toward the incipient primordium and an older primordium. Interestingly, the PIN1-GFP signal was highly reduced in the axillary region (arrowhead).

(C) and **(D)** Confocal image of an *AtPIN1:PIN1:GFP* tomato shoot apex after NPA treatment. NPA treatment led to an expansion of PIN1-GFP accumulation in the SAM (arrow).

(D) Close-up view of the axillary region of the apex shown in **(C)**. Different from the control shown in **(B)**, NPA-treated plants revealed PIN1-GFP accumulation in the axillary region (arrowhead), which was irregularly localized (arrow). Green indicates GFP protein fluorescence, whereas the red signal is caused by chlorophyll autofluorescence.

(E) and **(F)** PIN1 protein distribution in the Col-0 wild type **(E)** and the *pid-9* mutant **(F)**. Col-0 shows polar PIN1 localization (inset, arrowheads) in the L1 layer directed out of the axillary region (arrows). In *pid-9*, no polar PIN1 localization was observed. Arrow points to a leaf axil. Images are representative of multiple independent samples ($n > 10$). *Arabidopsis* materials were harvested from plants grown under SD for 28 d. Green indicates Alexa488 fluorescence, whereas the red signal is caused by chlorophyll auto fluorescence.

Bars = 50 μm in **(A)** and **(C)** and 20 μm in **(B)**, **(D)**, **(E)**, and **(F)**.

This finding is in agreement with previously published results (Bayer et al., 2009)

To investigate the effect of NPA treatment on AM formation, PIN1 distribution was also analyzed in tomato plants after watering with NPA. In these plants, PIN1 was highly expressed in young leaf primordia and in provascular elements (Figure 4C). Incipient leaf primordia were no longer detectable based on PIN1 localization. Instead, PIN1 expression was elevated in the whole SAM and no longer restricted to the L1 layer of the shoot apex. In the axillary region, PIN1 expression was low in comparison to the adjacent incipient leaf primordium. However, in comparison to control plants, PIN1 expression in leaf axils was strongly upregulated (Figures 4B and 4D). Furthermore, subcellular PIN1 localization and, as a consequence, its polarity in the leaf axil area was disturbed (Figure 4D; Supplemental Figures 5C and 5D).

To uncover possible species-specific differences in axillary auxin transport, we monitored PIN1 distribution in *Arabidopsis* shoot apices by immunofluorescence using an At-PIN1 antibody. In this species as in tomato, PIN1 proteins were detected in the L1 layer with an orientation pointing out from the leaf axil (Figure 4E). In contrast to the basal localization of PIN1 proteins reported for the inflorescence of *pid* mutants (Friml et al., 2004), we did not observe a regular intracellular polarization, but more a random distribution, of PIN1 proteins in the vegetative meristem of *pid-9* (Figure 4F). This finding may indicate a deviation in intracellular PIN1 polarization between the inflorescence and vegetative meristem of *pid* mutants.

Auxin Depletion Leads to Auxin Minima in Leaf Axils

PIN1 levels and polarization in the vicinity of leaf axils in tomato and *Arabidopsis* shoot apices indicated that the boundary zones of leaf primordia are likely depleted of auxin. To test this hypothesis, we monitored auxin signaling in leaf axils using the artificial auxin-responsive DR5 promoter. DR5, which has been widely used to monitor auxin responses (Ulmasov et al., 1997; Benková et al., 2003), contains several repeats of an auxin response element in conjunction with a minimal 35S promoter. Tomato plants harboring a *DR5:VENUS* construct (Shani et al., 2010) revealed a strong DR5:VENUS signal in incipient leaf primordia (P0) (Figure 5A), indicating a strong auxin response in this region. The signal expanded into the primordium during bulging, whereas it was reduced in the axillary region (Figure 5B). After leaf primordium outgrowth, but prior to the formation of leaflets, DR5:VENUS fluorescence was limited to the tip and the vasculature of the primordium and the signal in the leaf axil region dropped below detection (Figure 5C). Around the late P3/early P4 stage of leaf development, strong DR5:VENUS signals were detected on the adaxial side of leaf primordia, marking incipient leaflets and newly formed leaflets (Figure 5D). In the leaf axil region, no DR5 signal was detected at this stage.

As NPA treatment strongly changes PIN1 expression and localization in tomato leaf axils, we monitored its influence on auxin responses in this region. Both NPA- and mock-treated tomato plants showed strong DR5:VENUS signals at the position of incipient leaf primordia and at the tips of developing leaf primordia (Figures 5E and 5F). In contrast to the control, NPA-treated plants

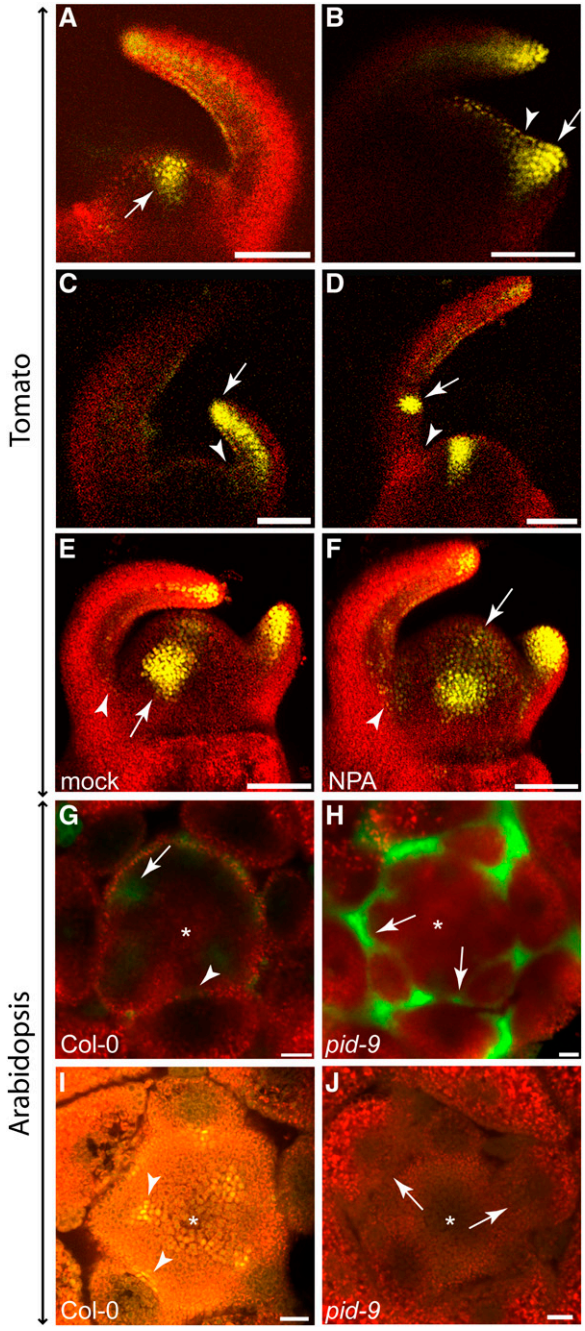

Figure 5. Auxin Signaling in Tomato and *Arabidopsis* Shoot Apices Monitored by Confocal Microscopy.

(A) to **(F)** Shoot apices of 14-d-old transgenic tomato plants (cv M82) expressing *DR5:VENUS*. Auxin response is reflected by VENUS fluorescence (yellow).

(A) DR5:VENUS signals were detected at positions of the incipient leaf primordia (arrow).

(B) After bulging of a new leaf primordium, its adaxial side was labeled (arrow), whereas DR5:VENUS signals were reduced in the axillary region (arrowhead).

(C) During primordium outgrowth, DR5:VENUS signals were detected at the tip and in the provascular traces of the primordium (arrow). In the leaf axil, no DR5:VENUS signals could be detected (arrowhead).

also revealed DR5:VENUS signals in the axillary region of the expanding leaf primordia extending into the apical meristem (Figure 5F). These data suggest that the adaxial boundary zone of leaf primordia is characterized by low auxin signaling.

To test this hypothesis in another plant species, the auxin response of leaf axils was analyzed in *Arabidopsis*. Sections through shoot apices of Col-0 *DR5:GFP* and *pid-9 DR5:GFP* plants were imaged by confocal microscopy. As presented in Figure 5G, the wild type displayed a strong DR5:GFP signal at the position where a new leaf primordium is initiated. Comparable to tomato, low DR5:GFP signals were found in the boundary zones of developing *Arabidopsis* leaf primordia (Figure 5G, arrow). However, in *pid-9*, strong DR5:GFP signals were found in leaf axils (Figure 5H, arrows), suggesting an elevated auxin response in *pid-9* leaf axils compared with the wild type.

An alternative auxin response sensor combines the AUX/IAA domain II, which is important for degradation of AUX/IAA repressors, with a nuclear-localized VENUS under the control of a 35S promoter (*DII-VENUS*). In the presence of auxin, DII-VENUS will be degraded by 26S proteasome and no DII-VENUS signal can be detected, whereas when auxin is absent, the DII-VENUS protein remains stable and can be detected (Brunoud et al., 2012). Transverse sections through shoot apices of Col-0 plants containing the *DII-VENUS* construct revealed strong VENUS signals in the boundary regions between the SAM and leaf primordia (Figure 5I). Interestingly, VENUS signals were detected mainly in the cells located in the center of these boundary regions, where new meristems will be formed, demonstrating low auxin levels or no auxin in these cells. By contrast, VENUS signals were not detectable in the boundary

(D) During leaf development, DR5:VENUS fluorescence was enhanced at positions where new leaflets were initiated (arrow). In the leaf axil, an auxin response was still not detectable at this stage (arrowhead).

(E) and **(F)** 3D reconstruction of mock- **(E)** and NPA-treated **(F)** *DR5:VENUS* tomato shoot apices. In mock-treated plants **(E)**, DR5:VENUS signals were absent from leaf axils (arrowhead) but present in incipient primordia (arrow), as well as in tips and the provascular strands of developing leaf primordia. After NPA treatment **(F)**, VENUS fluorescence could be detected in the axillary region (arrowhead) and was expanded in the SAM (arrow).

(G) and **(H)** Transverse sections through apices of transgenic Col-0 and *pid-9* plants expressing *DR5:GFP* (28 d in SD).

(G) In Col-0, strong DR5:GFP fluorescence was monitored in the incipient leaf primordia (arrow). No GFP signal was detectable in the leaf axil (arrowhead).

(H) In *pid-9*, GFP fluorescence was detected in the axillary region of leaf primordia (arrows).

(I) and **(J)** Transverse sections through apices of transgenic Col-0 and *pid-9* plants (28 d in SD) expressing *DII-VENUS*.

(I) In Col-0, DII-VENUS fluorescence signals were detected in axillary boundary zones (arrowheads), indicating low or no auxin levels in these regions.

(J) In *pid-9*, DII-VENUS fluorescence was not detectable in axillary regions (arrow), suggesting elevated auxin accumulation in these regions. Asterisks indicate the SAM.

Bars = 100 μm in **(A)** to **(F)** and 20 μm in **(G)** to **(J)**.

regions of *pid-9* apices (Figure 5J), suggesting high auxin accumulation, which corroborates the DR5:GFP results (Figure 5H).

An Auxin Minimum Is Required for Axillary Meristem Formation

As shown above, leaf axils are characterized by low auxin levels. This observation raises an important question: Are the auxin minima in leaf axils needed for AM initiation? To increase auxin levels in leaf axils, the axil-specific *LAS* promoter was fused to the bacterial auxin biosynthesis gene *iaaM* (Yamada et al., 1985) and introduced into the *Arabidopsis* wild type. Transgenic plants were analyzed for axillary bud formation. Several transgenic lines did not show a significant difference compared with untransformed control plants (Supplemental Figure 6). The failure to interfere with AM formation may be due to low activity of the *LAS* promoter. To increase the expression level of *iaaM*, two copies of the 35S enhancer element were added after the *LAS*-3′ region (*pLAS-en*). Transgenic plants carrying the *pLAS:iaaM-en* construct revealed significantly increased auxin levels in comparison to control plants (Supplemental Figure 7). *pLAS:iaaM-en* plants also exhibited several developmental defects. First, *pLAS:iaaM-en* plants displayed a dwarf growth habit with a reduced number of leaves (Figures 6A, 6B, and 6J). Furthermore, these plants were sterile, and inflorescences developed into a pin-like structure (Figure 6B). Importantly, *pLAS:iaaM-en* plants are compromised in forming axillary buds during vegetative development (Figures 6C and 6J). Side shoots developed only from the axils of late vegetative leaves. This result supports the view that an increase in auxin levels in the leaf axil region can disrupt AM formation.

AUX/IAA protein degradation plays an important role in auxin signal perception (Dharmasiri et al., 2005; Kepinski and Leyser, 2005; Weijers and Friml, 2009). However, specific mutations can stabilize AUX/IAA proteins and mediate a constitutive repression of auxin signaling (Hamann et al., 2002). A stabilized version of the AUX/IAA protein BODENLOS (BDL/IAA12) was generated by replacing proline-74 by serine and expressed from the *LAS* promoter (*pLAS:BDL-D*). This construct was supposed to repress auxin perception in the leaf axil region. Several independent *pLAS:BDL-D* lines initiated axillary buds in the axils of cotyledons, whereas Col-0 did not form such buds under the same conditions. When grown under short-day conditions for 6 weeks, these axillary buds developed into side shoots as tall as the main shoot (Figure 6D). Furthermore, if the 35S enhancer element was introduced (*pLAS:BDL-D-en*), transgenic plants developed as dwarfs, but produced more accessory side shoots (Figure 6F) and exhibited a bushier phenotype compared with wild-type plants (Figure 6E; Supplemental Figure 8), indicating that constitutive repression of auxin in leaf axils enhances side shoot formation.

As mentioned above, *pid-9* mutant plants exhibited strong branching defects, which may be a consequence of the elevated auxin responses in the leaf axils. To test this hypothesis, we introduced the *pLAS:BDL-D* construct into *pid-9* by crossing. Similar to *pid-9*, *pid-9 pLAS:BDL-D* plants formed pin-like inflorescences (Figure 6G). However, different from *pid-9*, the rosette leaf axils of *pid-9 pLAS:BDL-D* plants frequently formed axillary buds (Figures 6H to 6J), resulting in a significant increase in side shoot development (Figure 6K). Taken together, these results support the view that repression of auxin responses in the leaf axils of *pid-9* mutants can largely restore the formation of axillary buds.

DISCUSSION

Low Auxin Signaling Is a Hallmark of Boundary Zones

The plant hormone auxin has crucial functions in many developmental processes. At the vegetative shoot apex, polar auxin transport results in the formation of local auxin maxima, which coincides with the positions where leaf primordia are formed (Benková et al., 2003; Reinhardt et al., 2003). However, the adaxial boundary of leaf primordia, from which AMs develop, is characterized by low auxin levels, as suggested by the local distribution and polarization of the main auxin efflux carrier PIN1 (Figure 4) and the patterns of auxin response, monitored by the auxin sensors DR5:GFP and DII:VENUS (Figure 5) (Vernoux et al., 2011; Brunoud et al., 2012). How is this zone of low auxin response established? When a leaf primordium starts to grow out, intracellular polarization of PIN1 proteins in the adaxial boundary is reversed, from being polarized toward the primordium to being polarized toward the SAM (Figures 4 and 7) (Heisler et al., 2005). Plants lacking PIN1 activity are strongly compromised in AM initiation (Figure 2), even though the corresponding leaves can develop. This finding indicates that the process of AM formation is more sensitive to a loss of PIN1 activity than is leaf primordium initiation. Repolarization of PINs in the initiating boundary zone requires their activation by the PID kinase (Friml et al., 2004), which correlates well with expression of *PID* in the peripheral zone of the SAM (Figure 2). Loss of the PID kinase function results in accumulation of auxin in leaf axils (Figure 5). The partial complementation of the *pid* branching defect by specific expression of the *pLAS:BDL-D* construct suggests that the elevated auxin levels in the leaf axils of *pid* mutants are causal for the observed block in AM formation. After boundary zone establishment, PIN1 expression is downregulated in the leaf axil (Figure 4).

Boundary zones are characterized by specific expression of several transcriptional regulators, like *CUC* genes (Aida et al., 1997, 1999; Rast and Simon, 2008). Besides other readouts, these transcriptional regulators condition a retardation of growth in the boundary zone. Accumulation of auxin and expression of *CUC* genes in complementary domains of the embryonic shoot apex suggest that auxin negatively regulates expression of *CUC* genes (Furutani et al., 2004). With respect to boundary zone establishment, the leaf axil shows considerable similarity to the region between the cotyledons. These embryonic leaves initiate at the heart stage of embryo development, when PIN1 is polarized toward the positions where cotyledons will be formed. During this process, a strong DR5:GFP signal was detected at the incipient cotyledon primordia, whereas no signal could be detected in the boundary between cotyledons (Benková et al., 2003). This result led to the hypothesis that an auxin peak is needed to initiate cotyledon development, whereas formation of

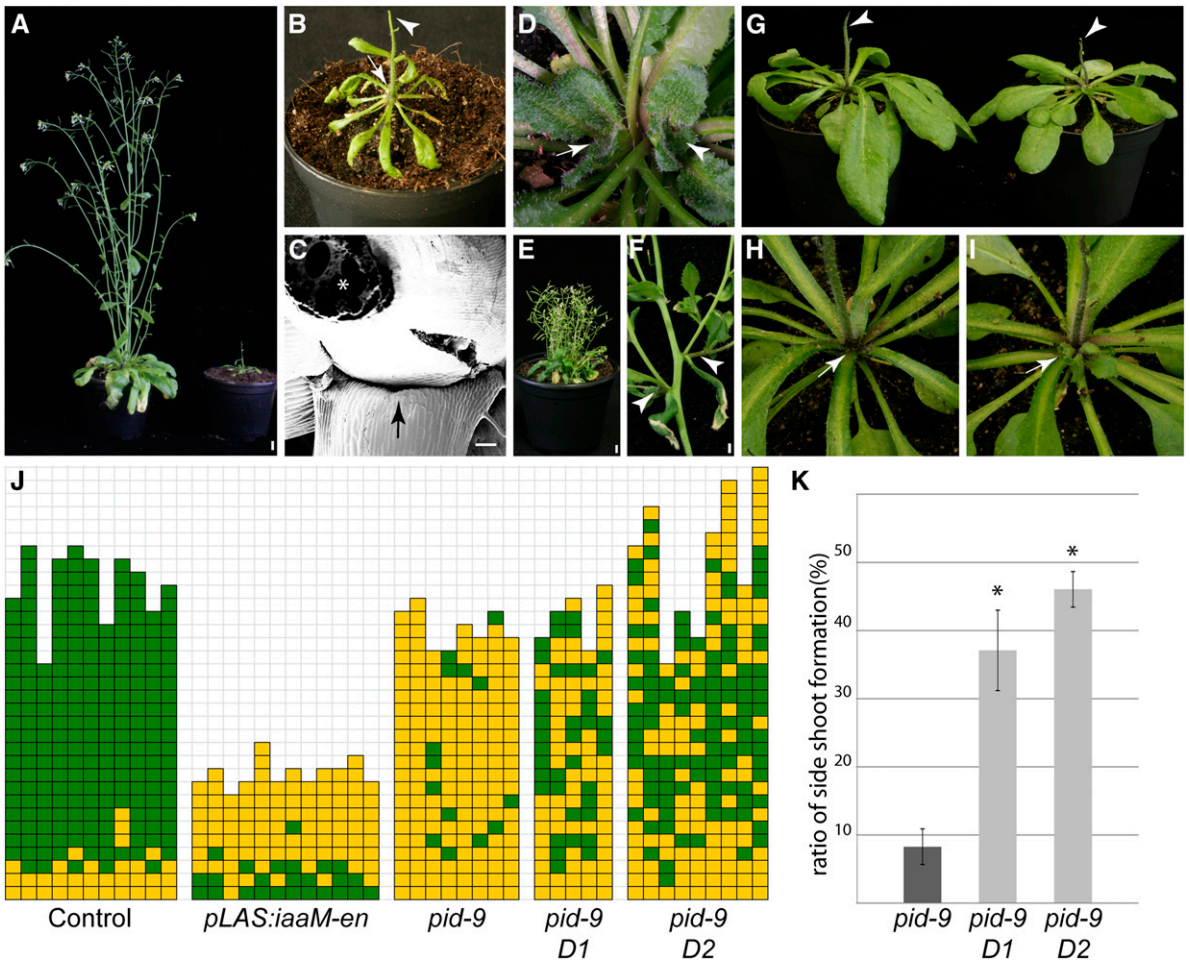

Figure 6. Auxin Depletion from the Leaf Axil Is Crucial for AM Formation.

(A) Growth habit of control (left) and *pLAS:iaaM-en* transgenic (right) plant.
(B) Close-up view of a *pLAS:iaaM-en* transgenic plants. Arrow points to the empty rosette leaf axils, and arrowhead points to a pin-like inflorescence.
(C) Scanning electron micrograph of a *pLAS:iaaM-en* plant. Arrow points to an empty leaf axil, and asterisk indicates the stem of the plant.
(D) Axillary bud developing in the cotyledon axil of a *pLAS:BDL-D* transgenic plants (20 out of 31). Arrow indicates the axillary bud, while arrowhead indicates the apical bud.
(E) *pLAS:BDL-D-en* plant exhibiting bushy stature.
(F) Accessory side shoot formation in *pLAS:BDL-D-en* plant (arrowhead).
(G) Growth habit of a *pid-9* mutant (left) and a *pid-9* mutant expressing *pLAS:BDL-D* (right). The pin-like inflorescence caused by the *pid-9* mutation was not rescued by expression of *pLAS:BDL-D* (arrowheads).
(H) Close-up of a *pid-9* mutant showing barren rosette leaf axils (arrow).
(I) Close-up of a transgenic *pid-9* plant expressing *pLAS:BDL-D*. Axillary bud formation is restored in several rosette leaf axils (arrow).
(J) Axillary bud formation in different plant populations. Genotypes are indicated below the column; two independent *pid-9* mutant lines carrying *pLAS:BDL-D* (*pid-9 D1* and *pid-9 D2*) were used. Green, bud/side shoot formation; yellow, empty leaf axils.
(K) Comparison of side shoot formation in rosette leaf axils of *pid-9* mutants to *pid-9 D1* and *pid-9 D2* (see **[J]**). Genotypes are indicated below the corresponding bars. Values represent means ± SE. Asterisk indicates statistically significant differences relative to *pid-9* ($P < 0.01$).
Plants were grown under SD for 4 weeks and shifted to LD for flower induction, with the exception of plants in **(D)**, which were grown under SD for 6 weeks. Bars = 1 cm in **(A)** and **(E)**, 100 μm in **(C)**, and 2 mm in **(F)**.

the SAM in the boundary between cotyledons requires a low auxin environment.

Recently, it has been demonstrated that a local auxin minimum is also required for establishment of the valve margin separation layer where opening of the *Arabidopsis* fruit occurs (Sorefan et al., 2009). The bHLH transcription factor INDEHISCENT coordinates auxin efflux from the separation layer. In all these developmental processes, boundary zones are crucial for the separation of different parts of the plant body, e.g., the two cotyledons or leaf and stem. Moreover, our results indicate that axillary boundary zones contain a pool of undifferentiated cells, which have the competence to form new meristems.

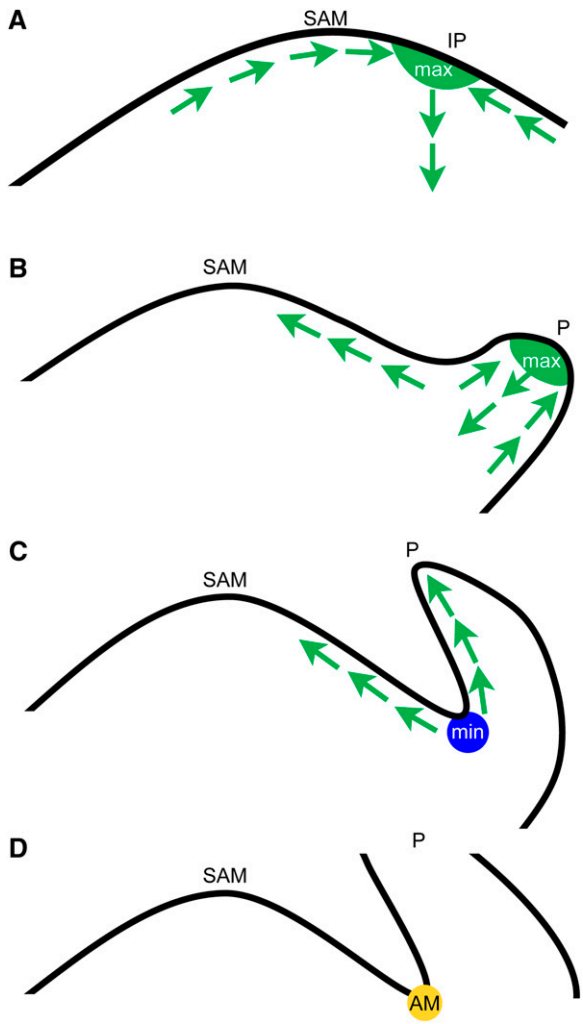

Figure 7. Model for Auxin Minimum Formation and Axillary Meristem Initiation.

(A) Convergent localization of PIN1 proteins leads to an auxin maximum (max, in green) where a new leaf primordium will form (IP).
(B) After the leaf primordium starts to grow, PIN1 will be localized toward the tip of the leaf primordium (P) and the SAM, and auxin gradients are generated.
(C) After leaf primordium elongation, auxin will be transported out of the axil region and an auxin minimum (min, blue circle) will form in the leaf axil.
(D) An AM (yellow circle) is formed in the low-auxin region. Arrows indicate PIN1-mediated auxin flux.

Low Auxin Signaling in Vegetative Leaf Axils Is Crucial to Condition Competence for AM Formation

Our data show that AMs originate from a zone that is characterized by low auxin levels. This result leads to the question of whether the low auxin environment is required for AM formation. We used two experimental approaches to alter auxin signaling in the leaf axil. Expression of an IAA auxin biosynthesis gene from the *LAS* promoter led to an increase in auxin level and to a strong reduction in axillary bud formation (Figure 6). On the other hand, expression of a stabilized version of the AUX/IAA protein BDL in the leaf axil was shown to complement the *pid* mutant phenotype. Furthermore, reduced auxin sensitivity, as found in the *axr1* mutant, leads to enhanced axillary bud formation (Stirnberg et al., 1999; Greb et al., 2003). From these data we conclude that a low auxin level in the leaf axil is a prerequisite for AM formation during *Arabidopsis* vegetative development.

However, recent reports have demonstrated that auxin response maxima promote the initiation of AMs during maize inflorescence development (Gallavotti et al., 2008). How can we explain these seemingly contradictory results? It is important to look at the timing of AM formation during development. During prolonged vegetative development in the *Arabidopsis* accession Col-0, AM formation can first be detected using the meristem marker *STM* in the 16th leaf axil (P16), counted from the SAM, and as a morphological structure in the axils of P21/P22 primordia (Greb et al., 2003). Similarly, in tomato (cv Moneymaker), AMs initiate in axils of P7 primordia (Supplemental Figure 4). Thus, during vegetative development, AM initiation is delayed with respect to formation of the subtending leaf primordium. However, at the transition to and during reproductive development AMs are formed together with or only slightly later than the supporting leaf primordium (Stirnberg et al., 1999, 2002). These observations indicate that AM formation is regulated by different mechanisms in the vegetative and reproductive phases. This view is supported by the pattern of axillary bud formation in loss-of-function mutants of *LAS* and *Ls*, key regulators of AM formation in *Arabidopsis* and tomato, respectively: *las*/*ls* mutants are compromised in AM initiation during vegetative development, but not in the reproductive phase (Greb et al., 2003). Mutations in several other regulators, like REGULATOR OF AXILLARY MERISTEMS1 (Müller et al., 2006) or REGULATOR OF AXILLARY MERISTEM FORMATION (Yang et al., 2012), also affect AM formation in the vegetative, but not in the reproductive phase of shoot development. *LAS*/*Ls*, which are expressed in the adaxial boundary of a leaf primordium from its initiation to AM formation (Greb et al., 2003), seem to be necessary only if AM formation is delayed. Similarly, depletion of auxin from leaf axils (Figure 7) may be specifically required to condition competence for AM formation during the vegetative phase of development. Taken together, this suggests that during prolonged vegetative development cells in the leaf axil need a special environment to establish or maintain their morphogenetic competence. In this context, low auxin levels could be part of a safeguard mechanism ensuring that leaf axil cells are not pushed into differentiation. This view is compatible with the detached meristem concept as proposed by Wardlaw (1943), who showed that in ferns, lateral buds originate from undifferentiated cell groups tracing back to the SAM. At the reproductive stage, such a mechanism is no longer needed because AMs initiate very rapidly in close proximity to the SAM. We cannot exclude that an auxin pulse, as observed for maize inflorescence development, is needed to trigger AM initiation. Nevertheless, our results show that auxin depletion from the boundary region between leaf primordia and the SAM is required to establish and maintain competence for AM formation.

METHODS

Plant Materials and Growth Conditions

Arabidopsis thaliana seeds were either obtained from the Nottingham Arabidopsis Stock Centre or from the authors who first described the line. All transgenic lines and mutants are in Col-0 (N1092) background unless stated otherwise. *Arabidopsis* lines used in this research are: *pid-9* (Christensen et al., 2000), *pin1* (Salk_47613), *aux lax1 lax2* (Bainbridge et al., 2008), *DR5er:GFP* (Benková et al., 2003), *DII-VENUS* (Brunoud et al., 2012), and *pid-8* (Ws-2) (Bennett et al., 1995). For cultivation under short-day (SD) conditions, *Arabidopsis* plants were grown in a controlled environment with an 8-h/16-h photoperiod, 25 to 15°C day-night temperature, and 60% relative humidity. Flowering was induced after 4 weeks by transferring the plants to a 16-h/8-h photoperiod. Cultivation under LD conditions was done in a conditioned greenhouse with additional artificial light when needed.

Tomato (*Solanum lycopersicum*) *AtPIN1:PIN1:GFP* (cv Moneymaker) and *DR5:VENUS* (cv M82) seeds were kindly provided by Cris Kuhlemeier and Naomi Ori, respectively. Tomato plants were grown under standard greenhouse conditions with additional artificial light (16-h/8-h photoperiod) when needed.

Axillary bud formation was analyzed after the onset of flowering using a stereomicroscope as previously described (Raman et al., 2008). Buds that had produced one or two leaf primordia as well as elongating side shoots were scored as leaf axils that had established axillary meristems. Selected samples were monitored by scanning electron microscopy to confirm the presence of barren leaf axils. All experiments were repeated at least once.

For NPA treatment, plants were either grown on medium containing 10 μM NPA (Supelco) or sprayed three times (48, 24, and 6 h) prior to analysis using 100 μM NPA and 0.02% Silwet-77.

DNA Construction and Transformation

DNA sequencing was performed by the MPIPZ service unit "Automatic DNA Isolation and Sequencing" using the 3730XL Genetic Analyzer (Applied Biosystems) or 3130XL Genetic Analyzer by means of BigDye terminator chemistry kit v3.1 (Applied Biosystems).

For *Arabidopsis*, *Agrobacterium tumefaciens*–mediated transformation was performed according to the floral dip method (Clough and Bent, 1998). To select for transgenic plants, T1 seedlings were sprayed with 250 mg/L glufosinate (BASTA; Hoechst) two to three times. Primer sequences and cloning strategies are listed in Supplemental Tables 1 and 2, respectively.

RNA in Situ Hybridization

Sample preparation and in situ hybridization of 8-μm sections was done as previously described by Coen et al. (1990) with slight modifications: 0.03% Tween 20 was added to the fixative, and dewatering of the fixed material was done without addition of $NaCl_2$. Plant material was embedded in Paraplast+ (Kendall) using the ASP300 tissue processor (Leica). Probes were not hydrolyzed. After the color reaction, slides were mounted in 30% glycerol and then imaged. The *PID* probe contained the nucleotide sequence from 822 to 1090 relative to start codon. *STM* and *LAS* probes were synthesized according to Greb et al. (2003) and the *WUS* probe according to Schulze et al. (2010). Plasmids for the *MP* probe were kindly provided by Cris Kuhlemeier, and the probe contained the nucleotides according to Hardtke and Berleth (1998). Linearized plasmids or PCR products were used as templates for *PID*, *STM*, *LAS*, and *WUS* antisense probes, and in vitro transcription was done by T7 RNA polymerase (Ambion). For *MP* probes, linearized plasmids were in antisense orientation relative to SP6 promoter in pSP72 vector. Probe syntheses were done using SP6 RNA polymerase (Roche).

Protein Localization Analysis

Sample preparation and immunohistobiochemistry procedures were performed as previously described by Paciorek et al. (2006) with some modifications. Tissues were fixed in methanol:acetic acid (v:v 3:1) overnight at −20°C and embedded in Paraplast+ (Kendall) using a ASP300 tissue processor (Leica). Eight-micrometer sections were made, and the wax removed by two treatments with Histoclear (National Diagnostics) for 10 min each. The primary antibody (Anti-AtPIN1; Santa Cruz) was diluted 1:500, and the secondary antibody (Alexa488-anti-goat; Invitrogen) was diluted 1:750. After the final washing step, sections were mounted in antifade (Invitrogen) and imaged by confocal microscopy.

Tomato apices were harvested by removing older leaves and fluorescence signals were monitored directly. For *Arabidopsis* vegetative shoot apices, plant tissues were collected, immediately placed in ice-cold 2.5% paraformaldehyde (PFA; Sigma-Aldrich) at pH 7.0 to 7.4, and vacuum infiltrated for ~30 min until all tissue ceased floating. The samples were transferred to fresh 2.5% PFA and stored at 4°C overnight. Next, the samples were washed with 10% sucrose (1% PFA, pH 7.0) for 20 min, 20% sucrose (1% PFA, pH 7.0) for 20 min, and finally with 30% sucrose (1% PFA, pH 7.0) for 30 min. Samples were then embedded in OCT (Sakura Finetek) at −20°C and 45- to 60-μm sections were made using a cryotome (Frigocut 2800; Reichert Jung). All selected sections were mounted with antifade (Invitrogen) and imaged by confocal microscopy.

Microscopy

Scanning electron microscopy was performed on a Supra 40 VP with a GEMINI column (Zeiss). Tissue was first frozen in liquid nitrogen and transferred to an Emitech K1250X for sublimation and subsequently coated with gold palladium before imaging. All images were obtained and processed using the SmartSEN software. In situ slides were imaged using an Axion-Plan2 stereomicroscope (Zeiss), and images of full plants were obtained using a MZ-16FA stereomicroscope (Leica). For the fluorescence images, Leica SP2, Leica SP8, or Zeiss LSM 700 confocal microscopes were used.

Analysis of Auxin

Auxin (IAA) was extracted, purified, and analyzed as previously described (Ruyter-Spira et al., 2011) with minor revisions. Samples of ~20 mg were extracted overnight at 4°C with 1 mL methanol containing [phenyl $^{13}C_6$]-IAA (0.02 nmol/mL) as internal standard. The methanol fraction was further purified by anion-exchange column (Grace Extra Clean Amino 100 mg/1.5 mL Solid Phase Extraction; Grace Davison Discovery Sciences). The volume of the wash and elution solvent was scaled down to 1 mL each to compensate for the reduced column size.

Statistical Analysis

When appropriate, data were subjected to the Student's *t* test (Microsoft Excel).

Accession Numbers

Sequence data from this article can be found in the Arabidopsis Genome Initiative or GenBank/EMBL databases under the following accession numbers: AT2G34650 (*PID*), AT1G73590 (*PIN1*), AT2G38120 (*AUX*), AT5G01240 (*LAX1*), AT2G21050 (*LAX2*), AT1G55580 (*LAS*), AT2G17950 (*WUS*), AT1G62360 (*STM*), AT1G19850 (*MP*), AT1G04550 (*BDL*), and M11035.1 (*iaaM*)

Supplemental Data

The following materials are available in the online version of this article.

Supplemental Figure 1. Mock and NPA-Treated Tomato Plants.

Supplemental Figure 2. Phenotype of *pid-8* Mutant Plants.

Supplemental Figure 3. *STM* and *LAS* Transcript Accumulation in Apices of *Arabidopsis* Wild-Type and *pid-9* Mutant Plants.

Supplemental Figure 4. Axillary Meristem Development in Tomato.

Supplemental Figure 5. PIN1 Localization in the Tomato Apex.

Supplemental Figure 6. *pLAS:iaaM* Plants Do Not Exhibit Strong Branching Defects.

Supplemental Figure 7. IAA Concentration in Control and *pLAS:iaaM-en* Plants.

Supplemental Figure 8. Comparison of a *pLAS:BDL-D-en* and a *pLAS:iaaM-en* Plant.

Supplemental Table 1. Primers.

Supplemental Table 2. Cloning Strategies.

ACKNOWLEDGMENTS

We thank Alexandra Kalde, Ursula Pfordt, Elmon Schmelzer, and Rainer Franzen (Max Planck Institute for Plant Breeding Research, Germany) for their technical assistance and Maarten Koornneef and Alice Hasson (MPIPZ, Germany) for critical reading of the article. We also thank Harro J. Bouwmeester and Tatsiana Charnikhova (Wageningen University, The Netherlands) for enabling auxin measurements. We thank Malcolm Bennett (University of Nottingham, UK), Csaba Koncz (MPIPZ, Germany), Cris Kuhlemeier (University of Bern, Switzerland), Paula McSteen (University of Missouri), and Naomi Ori (Hebrew University of Jerusalem, Israel) for kindly providing seeds and materials. This research was cosupported by the Alexander von Humboldt foundation (research fellowship 1146256 to W.K.). Research in the K.T. laboratory is in part funded by the Max-Planck-Society.

AUTHOR CONTRIBUTIONS

Q.W. and K.T. designed the research. Q.W., W.K., and S.R. performed the research. T.V. contributed a new analytic tool. Q.W., W.K., S.R., and K.T analyzed the data. Q.W., W.K., S.R., T.V., and K.T wrote the article.

Received January 15, 2014; revised April 18, 2014; accepted April 29, 2014; published May 21, 2014.

REFERENCES

Aida, M., Ishida, T., Fukaki, H., Fujisawa, H., and Tasaka, M. (1997). Genes involved in organ separation in Arabidopsis: an analysis of the cup-shaped cotyledon mutant. Plant Cell **9:** 841–857.

Aida, M., Ishida, T., and Tasaka, M. (1999). Shoot apical meristem and cotyledon formation during Arabidopsis embryogenesis: interaction among the CUP-SHAPED COTYLEDON and SHOOT MERISTEMLESS genes. Development **126:** 1563–1570.

Bainbridge, K., Guyomarc'h, S., Bayer, E., Swarup, R., Bennett, M., Mandel, T., and Kuhlemeier, C. (2008). Auxin influx carriers stabilize phyllotactic patterning. Genes Dev. **22:** 810–823.

Bayer, E.M., Smith, R.S., Mandel, T., Nakayama, N., Sauer, M., Prusinkiewicz, P., and Kuhlemeier, C. (2009). Integration of transport-based models for phyllotaxis and midvein formation. Genes Dev. **23:** 373–384.

Benková, E., Michniewicz, M., Sauer, M., Teichmann, T., Seifertová, D., Jürgens, G., and Friml, J. (2003). Local, efflux-dependent auxin gradients as a common module for plant organ formation. Cell **115:** 591–602.

Bennett, S.R.M., Alvarez, J., Bossinger, G., and Smyth, D.R. (1995). Morphogenesis in *pinoid* mutants of *Arabidopsis thaliana.* Plant J. **8:** 505–520.

Brunoud, G., Wells, D.M., Oliva, M., Larrieu, A., Mirabet, V., Burrow, A.H., Beeckman, T., Kepinski, S., Traas, J., Bennett, M.J., and Vernoux, T. (2012). A novel sensor to map auxin response and distribution at high spatio-temporal resolution. Nature **482:** 103–106.

Busch, B.L., Schmitz, G., Rossmann, S., Piron, F., Ding, J., Bendahmane, A., and Theres, K. (2011). Shoot branching and leaf dissection in tomato are regulated by homologous gene modules. Plant Cell **23:** 3595–3609.

Christensen, S.K., Dagenais, N., Chory, J., and Weigel, D. (2000). Regulation of auxin response by the protein kinase PINOID. Cell **100:** 469–478.

Clough, S.J., and Bent, A.F. (1998). Floral dip: a simplified method for *Agrobacterium*-mediated transformation of *Arabidopsis thaliana.* Plant J. **16:** 735–743.

Coen, E.S., Romero, J.M., Doyle, S., Elliott, R., Murphy, G., and Carpenter, R. (1990). floricaula: a homeotic gene required for flower development in antirrhinum majus. Cell **63:** 1311–1322.

Dharmasiri, N., Dharmasiri, S., and Estelle, M. (2005). The F-box protein TIR1 is an auxin receptor. Nature **435:** 441–445.

Evans, M.W., and Grover, F.O. (1940). Developmental morphology of the growing point of the shoot and the inflorescence in grasses. J. Agric. Res. **61:** 481–520.

Friml, J., et al. (2004). A PINOID-dependent binary switch in apical-basal PIN polar targeting directs auxin efflux. Science **306:** 862–865.

Furutani, M., Vernoux, T., Traas, J., Kato, T., Tasaka, M., and Aida, M. (2004). PIN-FORMED1 and PINOID regulate boundary formation and cotyledon development in Arabidopsis embryogenesis. Development **131:** 5021–5030.

Gallavotti, A., Yang, Y., Schmidt, R.J., and Jackson, D. (2008). The Relationship between auxin transport and maize branching. Plant Physiol. **147:** 1913–1923.

Gälweiler, L., Guan, C., Müller, A., Wisman, E., Mendgen, K., Yephremov, A., and Palme, K. (1998). Regulation of polar auxin transport by AtPIN1 in Arabidopsis vascular tissue. Science **282:** 2226–2230.

Gomez-Roldan, V., et al. (2008). Strigolactone inhibition of shoot branching. Nature **455:** 189–194.

Grbić, V., and Bleecker, A.B. (2000). Axillary meristem development in *Arabidopsis thaliana*. Plant J. **21:** 215–223.

Greb, T., Clarenz, O., Schäfer, E., Müller, D., Herrero, R., Schmitz, G., and Theres, K. (2003). Molecular analysis of the *LATERAL SUPPRESSOR* gene in *Arabidopsis* reveals a conserved control mechanism for axillary meristem formation. Genes Dev. **17:** 1175–1187.

Hamann, T., Benkova, E., Bäurle, I., Kientz, M., and Jürgens, G. (2002). The Arabidopsis BODENLOS gene encodes an auxin response protein inhibiting MONOPTEROS-mediated embryo patterning. Genes Dev. **16:** 1610–1615.

Hardtke, C.S., and Berleth, T. (1998). The Arabidopsis gene MONOPTEROS encodes a transcription factor mediating embryo axis formation and vascular development. EMBO J. **17:** 1405–1411.

Heisler, M.G., Ohno, C., Das, P., Sieber, P., Reddy, G.V., Long, J.A., and Meyerowitz, E.M. (2005). Patterns of auxin transport and gene expression during primordium development revealed by live imaging of the Arabidopsis inflorescence meristem. Curr. Biol. **15:** 1899–1911.

Hempel, F., and Feldman, L. (1994). Bi-directional inflorescence development in *Arabidopsis thaliana*: Acropetal initiation of flowers and basipetal initiation of paraclades. Planta **192:** 276–286.

Hibara, K., Karim, M.R., Takada, S., Taoka, K., Furutani, M., Aida, M., and Tasaka, M. (2006). Arabidopsis *CUP-SHAPED COTYLEDON3* regulates postembryonic shoot meristem and organ boundary formation. Plant Cell **18:** 2946–2957.

Kepinski, S., and Leyser, O. (2005). The Arabidopsis F-box protein TIR1 is an auxin receptor. Nature **435:** 446–451.

Koenig, D., Bayer, E., Kang, J., Kuhlemeier, C., and Sinha, N. (2009). Auxin patterns *Solanum lycopersicum* leaf morphogenesis. Development **136:** 2997–3006.

Laux, T., and Jurgens, G. (1997). Embryogenesis: a new start in life. Plant Cell **9:** 989–1000.

Leyser, H.M.O., Lincoln, C.A., Timpte, C., Lammer, D., Turner, J., and Estelle, M. (1993). Arabidopsis auxin-resistance gene AXR1 encodes a protein related to ubiquitin-activating enzyme E1. Nature **364:** 161–164.

Li, X., et al. (2003). Control of tillering in rice. Nature **422:** 618–621.

Lincoln, C., Britton, J.H., and Estelle, M. (1990). Growth and development of the *axr1* mutants of Arabidopsis. Plant Cell **2:** 1071–1080.

Long, J., and Barton, M.K. (2000). Initiation of axillary and floral meristems in Arabidopsis. Dev. Biol. **218:** 341–353.

Mayer, K.F.X., Schoof, H., Haecker, A., Lenhard, M., Jürgens, G., and Laux, T. (1998). Role of WUSCHEL in regulating stem cell fate in the Arabidopsis shoot meristem. Cell **95:** 805–815.

McSteen, P., and Hake, S. (2001). *barren inflorescence2* regulates axillary meristem development in the maize inflorescence. Development **128:** 2881–2891.

McSteen, P., Malcomber, S., Skirpan, A., Lunde, C., Wu, X., Kellogg, E., and Hake, S. (2007). barren inflorescence2 Encodes a co-ortholog of the PINOID serine/threonine kinase and is required for organogenesis during inflorescence and vegetative development in maize. Plant Physiol. **144:** 1000–1011.

Michniewicz, M., et al. (2007). Antagonistic regulation of PIN phosphorylation by PP2A and PINOID directs auxin flux. Cell **130:** 1044–1056.

Müller, D., Schmitz, G., and Theres, K. (2006). Blind homologous R2R3 Myb genes control the pattern of lateral meristem initiation in Arabidopsis. Plant Cell **18:** 586–597.

Okada, K., Ueda, J., Komaki, M.K., Bell, C.J., and Shimura, Y. (1991). Requirement of the auxin polar transport system in early stages of Arabidopsis floral bud formation. Plant Cell **3:** 677–684.

Paciorek, T., Sauer, M., Balla, J., Wiśniewska, J., and Friml, J. (2006). Immunocytochemical technique for protein localization in sections of plant tissues. Nat. Protoc. **1:** 104–107.

Raman, S., Greb, T., Peaucelle, A., Blein, T., Laufs, P., and Theres, K. (2008). Interplay of miR164, *CUP-SHAPED COTYLEDON* genes and *LATERAL SUPPRESSOR* controls axillary meristem formation in *Arabidopsis thaliana.* Plant J. **55:** 65–76.

Rast, M.I., and Simon, R. (2008). The meristem-to-organ boundary: more than an extremity of anything. Curr. Opin. Genet. Dev. **18:** 287–294.

Reinhardt, D., Pesce, E.R., Stieger, P., Mandel, T., Baltensperger, K., Bennett, M., Traas, J., Friml, J., and Kuhlemeier, C. (2003). Regulation of phyllotaxis by polar auxin transport. Nature **426:** 255–260.

Ruyter-Spira, C., Kohlen, W., Charnikhova, T., van Zeijl, A., van Bezouwen, L., de Ruijter, N., Cardoso, C., Lopez-Raez, J.A., Matusova, R., Bours, R., Verstappen, F., and Bouwmeester, H. (2011). Physiological effects of the synthetic strigolactone analog GR24 on root system architecture in Arabidopsis: another belowground role for strigolactones? Plant Physiol. **155:** 721–734.

Schmitz, G., and Theres, K. (2005). Shoot and inflorescence branching. Curr. Opin. Plant Biol. **8:** 506–511.

Schulze, S., Schäfer, B.N., Parizotto, E.A., Voinnet, O., and Theres, K. (2010). *LOST MERISTEMS* genes regulate cell differentiation of central zone descendants in Arabidopsis shoot meristems. Plant J. **64:** 668–678.

Schumacher, K., Schmitt, T., Rossberg, M., Schmitz, G., and Theres, K. (1999). The *Lateral suppressor* (*Ls*) gene of tomato encodes a new member of the VHIID protein family. Proc. Natl. Acad. Sci. USA **96:** 290–295.

Shani, E., Ben-Gera, H., Shleizer-Burko, S., Burko, Y., Weiss, D., and Ori, N. (2010). Cytokinin regulates compound leaf development in tomato. Plant Cell **22:** 3206–3217.

Sorefan, K., Girin, T., Liljegren, S.J., Ljung, K., Robles, P., Galván-Ampudia, C.S., Offringa, R., Friml, J., Yanofsky, M.F., and Østergaard, L. (2009). A regulated auxin minimum is required for seed dispersal in Arabidopsis. Nature **459:** 583–586.

Stirnberg, P., Chatfield, S.P., and Leyser, H.M. (1999). AXR1 acts after lateral bud formation to inhibit lateral bud growth in *Arabidopsis.* Plant Physiol. **121:** 839–847.

Stirnberg, P., van De Sande, K., and Leyser, H.M.O. (2002). MAX1 and MAX2 control shoot lateral branching in Arabidopsis. Development **129:** 1131–1141.

Takada, S., Hibara, K., Ishida, T., and Tasaka, M. (2001). The CUP-SHAPED COTYLEDON1 gene of Arabidopsis regulates shoot apical meristem formation. Development **128:** 1127–1135.

Thimann, K.V., and Skoog, F. (1934). On the inhibition of bud development and other functions of growth substance in *Vicia faba*. Proc. R. Soc. Lond. B Biol. Sci. **114:** 317–339.

Ulmasov, T., Murfett, J., Hagen, G., and Guilfoyle, T.J. (1997). Aux/IAA proteins repress expression of reporter genes containing natural and highly active synthetic auxin response elements. Plant Cell **9:** 1963–1971.

Umehara, M., Hanada, A., Yoshida, S., Akiyama, K., Arite, T., Takeda-Kamiya, N., Magome, H., Kamiya, Y., Shirasu, K., Yoneyama, K., Kyozuka, J., and Yamaguchi, S. (2008). Inhibition of shoot branching by new terpenoid plant hormones. Nature **455:** 195–200.

Vernoux, T., Besnard, F., and Traas, J. (2010). Auxin at the shoot apical meristem. Cold Spring Harb. Perspect. Biol. **2:** a001487.

Vernoux, T., et al. (2011). The auxin signalling network translates dynamic input into robust patterning at the shoot apex. Mol. Syst. Biol. **7:** 508.

Vroemen, C.W., Mordhorst, A.P., Albrecht, C., Kwaaitaal, M.A.C.J., and de Vries, S.C. (2003). The CUP-SHAPED COTYLEDON3 gene is required for boundary and shoot meristem formation in Arabidopsis. Plant Cell **15:** 1563–1577.

Wardlaw, C.W. (1943). Experimental and analytical studies of Pteridophytes. I. Preliminary observations on the development of buds on the rhizome of the ostrich fern (*Matteuccia struthiopteris* Tod.). Ann. Bot. (Lond.) **26:** 171–187.

Weijers, D., and Friml, J. (2009). SnapShot: auxin signaling and transport. Cell **136:** 1172–1172.

Wu, X., and McSteen, P. (2007). The role of auxin transport during inflorescence development in maize (*Zea mays*, Poaceae). Am. J. Bot. **94:** 1745–1755.

Yamada, T., Palm, C.J., Brooks, B., and Kosuge, T. (1985). Nucleotide sequences of the *Pseudomonas savastanoi* indoleacetic acid genes show homology with *Agrobacterium tumefaciens* T-DNA. Proc. Natl. Acad. Sci. USA **82:** 6522–6526.

Yang, F., Wang, Q., Schmitz, G., Müller, D., and Theres, K. (2012). The bHLH protein ROX acts in concert with RAX1 and LAS to modulate axillary meristem formation in Arabidopsis. Plant J. **71:** 61–70.

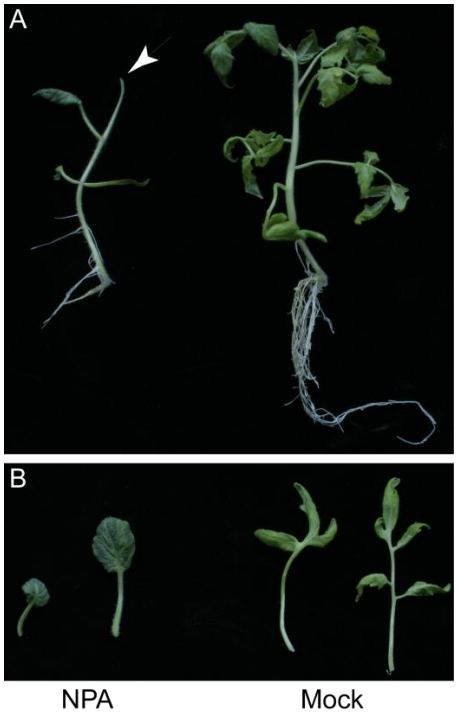

Supplemental Figure1: Mock and NPA-treated tomato plants.
(A) NPA treated tomato (cv. Moneymaker) developed a pin-like inflorescence (arrowhead). (B) Comparison of first and second leaves from mock and NPA treated tomato plants. NPA-treated plants had simpler leaves.

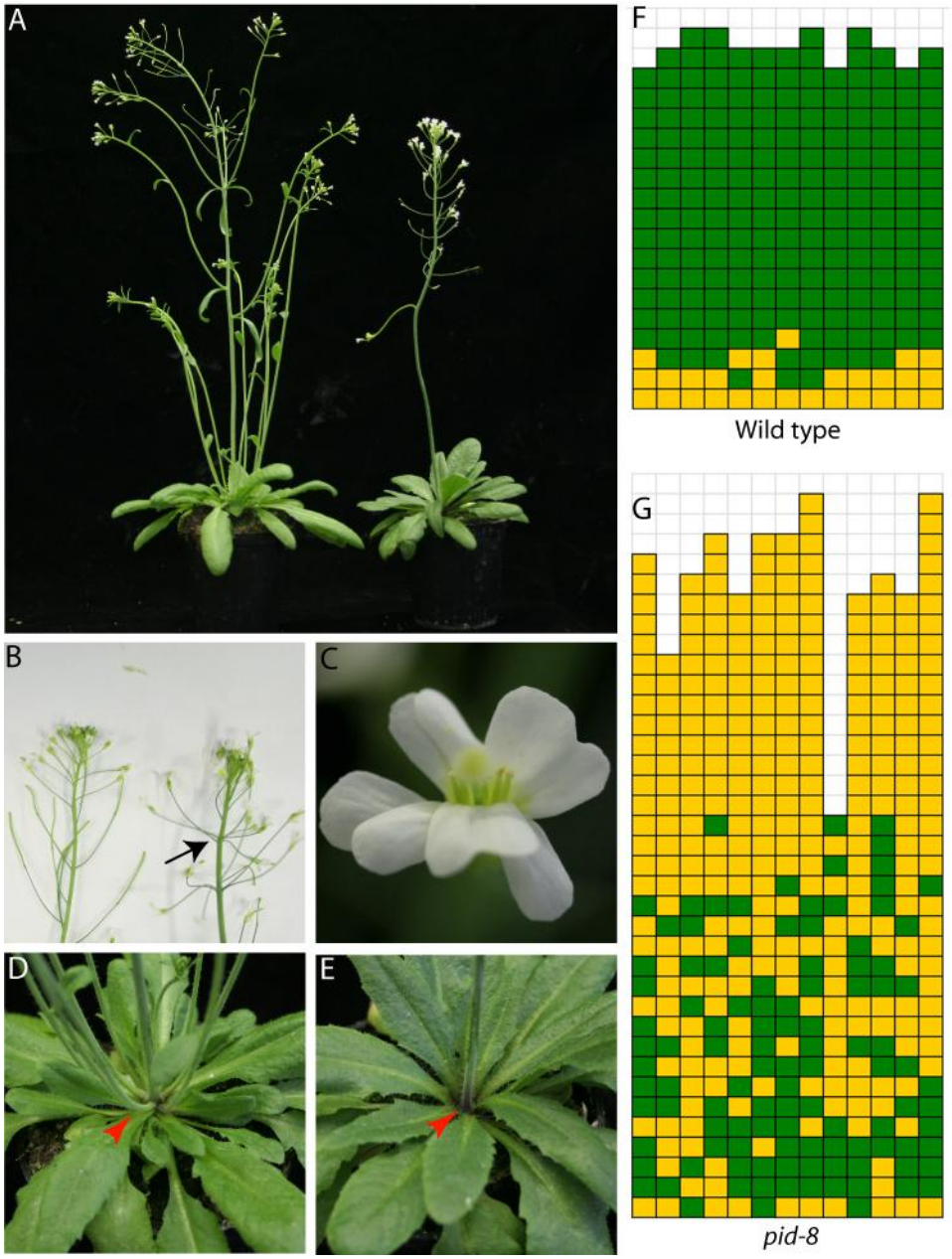

Supplemental Figure 2: Phenotype of *pid-8* mutant plants.
(A) Habitus of a Ws wild type plant (left) and a *pid-8* mutant (right). Plants were grown for 28 days under SD conditions and then shifted to LD to induce flowering. (B) Comparison of an inflorescence between Ws (left) and *pid-8* (right), arrow points to a cluster of flowers. (D) Close-up view of a *pid-8* flower. (D, E) Close-up view of a Ws and a *pid-8* rosette. In Ws, side shoots are formed (D, arrowhead) while in *pid-8* most leaf axils are empty (E, arrowhead). (F-G) Schematic representation of axillary bud formation in rosette leaf axils of *pid-8* (G) in comparison to the Ws wild type (F, n=13). Plants were grown for 28 days under SD conditions and then shifted to LD to induce flowering. Each column represents a single plant and each square within a column representing an individual leaf axil. The bottom row represents the oldest rosette leaf axils, with positions of progressively younger rosette leaves on top of it. Green denotes the presence of an axillary bud and yellow the absence of an axillary bud in any particular leaf axil.

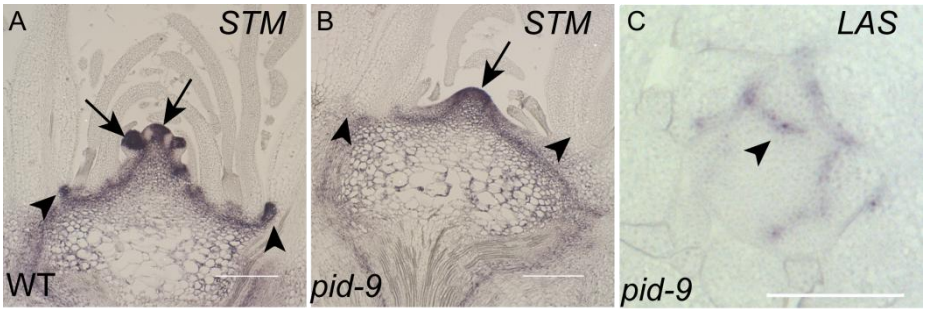

Supplemental Figure 3: *STM* and *LAS* transcript accumulation in apices of Arabidopsis wild type and *pid-9* mutant plants.
(A, B) Longitudinal sections through shoot apices of Col-0 wild type (A) and *pid-9* (B) plants were hybridized with a *STM* antisense probe. Sections were prepared from plants grown under SD conditions for 28 days and shift to LD for 7 days before fixation. In both wild type and *pid-9* plants, *STM* mRNA is detected in the inflorescence meristem and interprimodial regions (A and B, arrows). Focused *STM* expression domains in older leaf axils was present in wild type but absent in *pid-9* (A and B, arrowheads). In addition, *pid-9* plants did not form any floral meristems and the main meristem was naked (B). (C) Transverse section through the shoot tip of *pid-9* plant was hybridized with a probe from the *LAS* gene, arrowhead indicates that *LAS* was expressed at the boundary between the SAM and leaf primordia. Probes are indicated in the upper right corner, genotypes are indicated in the bottom left corner. Scale bars: A and B 200 μm; C 100 μm.

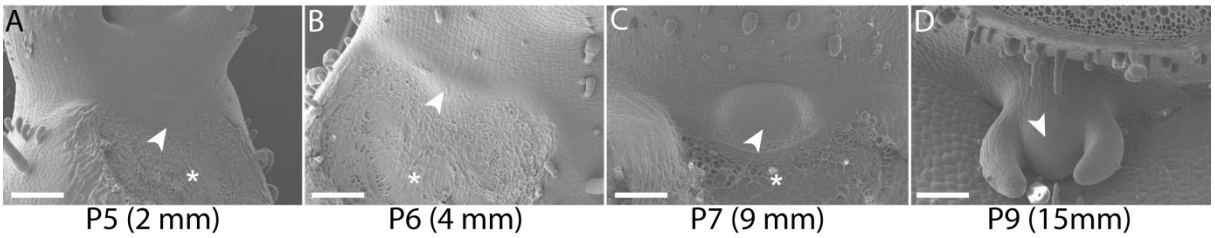

Supplemental Figure 4: Axillary meristem development in tomato.
(A-D) AM initiation was studied by SEM micrographs of young leaf axils from wild type tomato plants (cv. Moneymaker). Primordia of different sizes (2-9 mm) were removed from two-week-old tomato seedlings (marked with asterisks (*)) to monitor morphological changes. Arrowheads point to an empty leaf axil (A), developing AMs (B and C) and to an axillary bud (D). Scale bars: 100 μm.

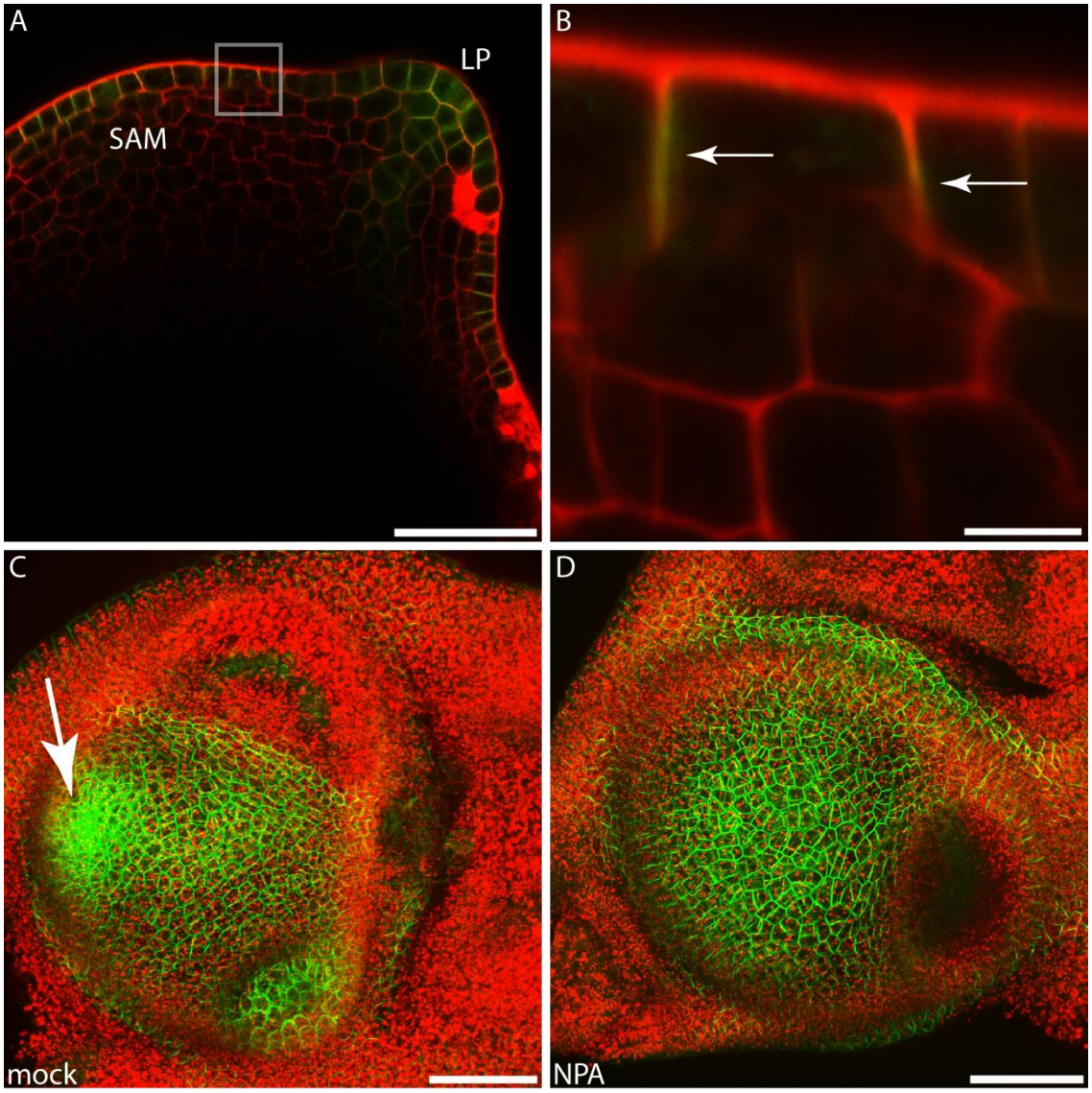

Supplemental Figure 5: PIN1 localization in the tomato apex.
(A) Confocal image of a tomato apex with PIN1-GFP construct. LP (leaf primordium), SAM (shoot apical meristem). (B) Close-up view of region marked in A, arrow indicate polarity of auxin flux. (C, D) 3D reconstruction of PIN1-GFP tomato apex with mock (C) and NPA (D) treatment. In C the arrow points to the incipient leaf primordium. Scale bars: A 50 µm, B 5 µm, C and D 100 µm. Green indicates GFP signal, red indicates Propidium Iodide (PI, Sigma-Aldrich, USA) stained cell walls (A, B) or chlorophyll auto fluorescence (C, D).

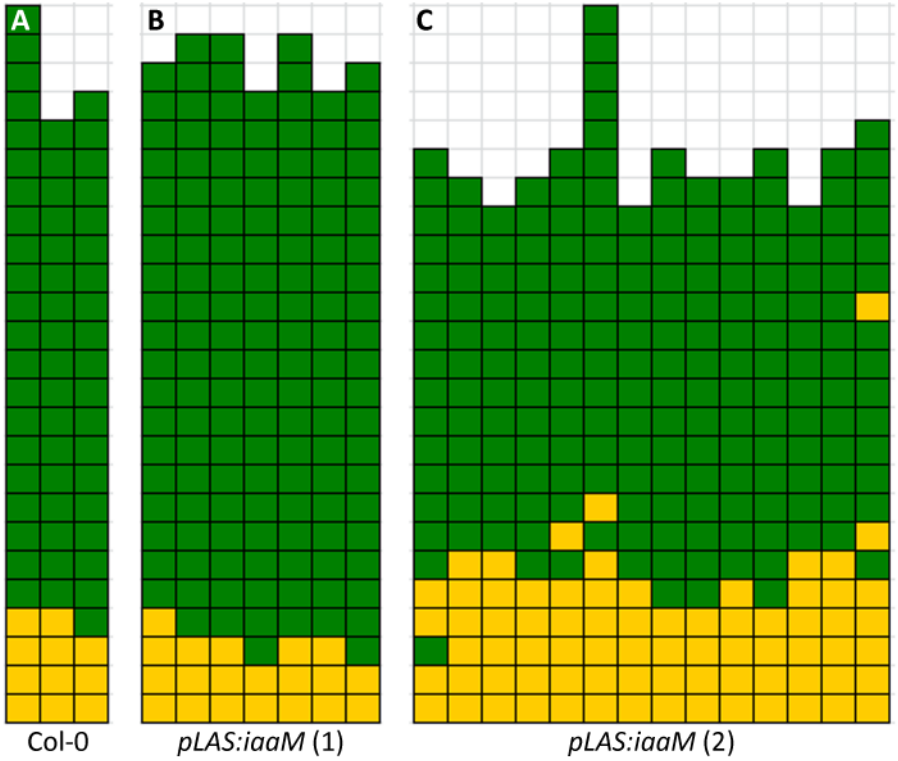

Supplemental Figure 6: *pLAS:iaaM* plants do not exhibit strong branching defects.
(A-C) Schematic representation of axillary bud formation in rosette leaf axils of Col-0 wild type (A, n=3) in comparison to two different *pLAS:iaaM* transgenic lines (B, n=7; C, n=14). Plants were grown under SD conditions for 28 days and then shifted to LD to induce flowering. Each column represents a single plant, with each square within a column representing an individual leaf axil. The bottom row represents the oldest rosette leaf axils, with positions of progressively younger rosette leaves on top of it. Green denotes the presence of an axillary bud and yellow the absence of an axillary bud in any particular leaf axil.

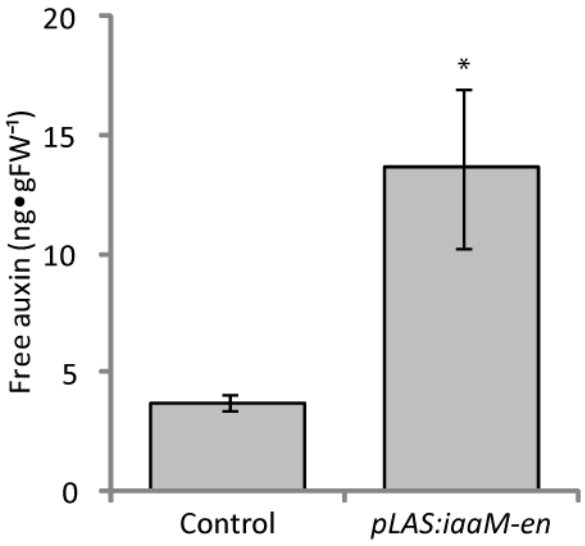

Supplemental Figure 7: IAA concentration in control and *pLAS:iaaM-en* plants.
Bars indicate average level of free auxin in 2-week-old seedlings (± SE, n=6). Asterisk (*) indicates statistically significant differences relative to control ($p < 0.05$).

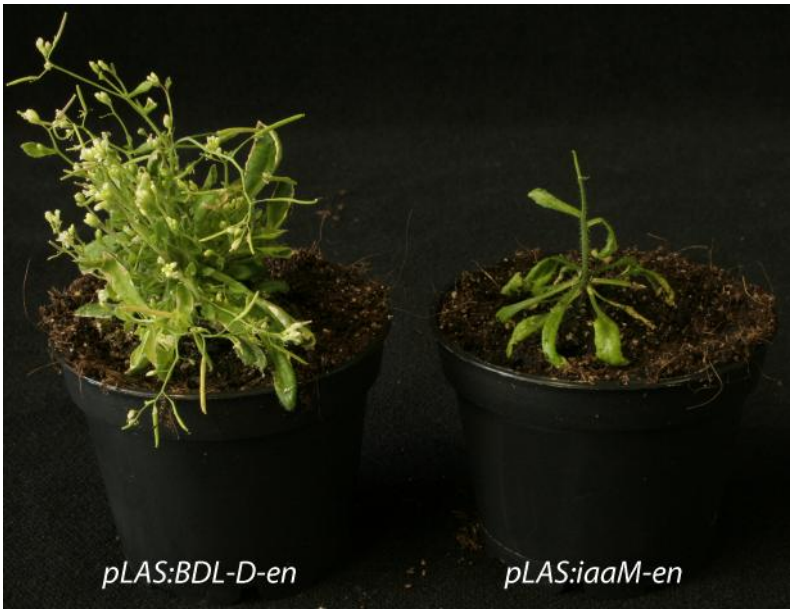

Supplemental Figure 8: Habitus of a *pLAS:BDL-D-en* plant (left) and a *pLAS:iaaM-en* plant (right). Plants were grown for 28 days under SD conditions and then shifted to LD to induce flowering. Images are representative of multiple plants (n>10).

Supplemental Table 1. Primers

pid-ish 5'	ACCAACCCGTCTCTTTGTTG	*PID* probe
pid-ish 3'-T7	TAATACGACTCACTATAGGGAGAGCGCATGAAGCTCAAACATA	*PID* probe
pid-ish 3'	GCGCATGAAGCTCAAACATA	*PID* probe
pid phenotype R	ACTAGAACTTCGGCGGCATA	*pid-9* genotype
GABI left	ATATTGACCATCATACTCATTGC	*pid-9* genotype
LB b1	GCGTGGACCGCTTGCTGCAACT	*pin1*genotype
pin1 47613 R	AGCATGCTTTCTGCTGTGAA	*pin1*genotype
pin1 47613 F	TAAGGTGATGCCACCAACAA	*pin1*genotype
BDLfor1Acc65I	CGTGGTACCATGCGTGGTGTGTCAGAA	*BDL* cloning
BDLRev1AvrII	CGTCCTAGGCTAAACAGGGTTGTTTCT	*BDL* cloning
BDLrev2mut	TGGTGACCATCCTACCACTTG	*BDL* mutation
BDLfor2mut	CAAGTGGTAGGATGGTCACCA	*BDL* mutation
iM1f-iaaMfor1Acc65I	CGTGGTACCATGTATGACCATTTTAATTCA	*iaaM* cloning
iM1r-iaaMrev1AvrII	CGTCCTAGGTTAATAGCGATAGGAGGCGTT	*iaaM* cloning
pid-EcoRI F	TAAGAATTCATGTTACGAGAATCAGAC	*pid-9* genotype
PlasmidF	CACGACGTTGTAAAACGACGGCCAG	*LAS* promoter cloning
AE42-1522R	CATCCTAGGCATGGTACCTTGAAACGATAGAAAAAGATG	*LAS* promoter cloning
35enhan-NotIF	CATGCGGCCGCATCACATCAATCCACTTG	2x35S enhancer cloning
35enhan-NotIR	CATGCGGCCGCAACATGGTGGAGCACGAC	2x35S enhancer cloning

Supplemental Table 2. Cloning strategies

Use	Construct	Plasmid name	Insert or PCR product	Primers	Template	Plasmid backbone	Cloning method
Cloning vector	*LAS* 5' and 3' promoter (*LAS*)	pSR40	1447 bp of 5' and 4564 bp of 3' promoter	PlasmidF + AE42-1522R	pAE421[1]	pGEM	aa site
Cloning vector	*pLAS:iaaM*	pQW17	*iaaM* ORF	iM1f-iaaMfor1Acc65I + iM1r-iaaMrev1AvrII	*iaaM* construct kindly provided by Csaba Koncz	pSR40	Acc65I / AvrII
Cloning vector	*pLAS:BDL-D*	pQW19	C200 to T200 mutated *BDL* ORF	Two-step PCR:		pSR40	Acc65I / AvrII
				(1) (a) BDLfor1Acc65I + BDLrev2mut (b) BDLfor2mut + BDLRev1AvrII	Arabidopsis cDNA		
				(2) BDLfor1Acc65I + BDLRev1AvrII	Purified PCR products pooled from (1)		
for Arabidopsis transformation	*pLAS:iaaM*	pQW22	pQW17	-	-	pGPTV-Bar-AscI[2]	AscI
for Arabidopsis transformation	*pLAS:BDL-D*	pQW24	pQW19	-	-	pGPTV-Bar-AscI[2]	AscI
Cloning vector	*pLAS:iaaM-en*	pQW58	2x35s enhancer	35enhan-NotIF + 35enhan-NotIR	described in Busch et al. (2011)	pQW17	NotI
for Arabidopsis transformation	*pLAS:iaaM-en*	pQW62	pQW58	-	-	pGPTV-Bar-AscI[2]	AscI
Cloning vector	*pLAS:BDL-D-en*	pQW59	2x35s enhancer	35enhan-NotIF + 35enhan-NotIR	described in Busch et al. (2011)	pQW19	NotI
for Arabidopsis transformation	*pLAS:BDL-D-en*	pQW63	pQW59	-	-	pGPTV-Bar-AscI[2]	AscI

[1] Eicker (2005)
[2] Überlacker and Werr (1996)

Supplemental References:

Busch, B.L., Schmitz, G., Rossmann, S., Piron, F., Ding, J., Bendahmane, A., and Theres, K. (2011). Shoot branching and leaf dissection in tomato are regulated by homologous gene modules. Plant Cell **23,** 3595-3609.

Eicker, A. (2005). Studien zur Charakterisierung der regulatorischen Elemente des LATERAL SUPPRESSOR Gens in Arabidopsis thaliana. Inaugural-Dissertation, Universität zu Köln.

Überlacker, B., and Werr, W. (1996). Vectors with rare-cutter restriction enzyme sites for expression of open reading frames in transgenic plants. Mol Breeding **2,** 293-295.